Supporting Information

Environmentally persistent free radicals readily form on TiO$_2$ but not on ZnO nanoparticles

Thermal system for synthesizing radicals. The main part of the setup consisted of a glass chamber as the reactor. We used this chamber for equilibrating the vaporized organic precursor (**Fig.** S1A). The equilibration chamber consisted of an injection port (**Fig.** S1B), two ports for attaching the EPFR reactor vessels, and an outlet for pulling a vacuum. Regions heated >250 °C, such as the EPFR reactor vessels, were made of quartz to reduce unwanted side reactions with the glass walls, while the rest were borosilicate glass. The EPFR reaction tube, the section of the setup where EPFRs are formed, is depicted in **Fig.** S1C**.** The EPFR reaction tube was a long-stemmed quartz reactor with a spherical protrusion of ~1 inch to contain the NPs. We attached a detachable ESR tube as a sidearm to collect samples before electron spin resonance (ESR) measurement. We heat only the bulbous portion where the dosing of the organic adsorbates took place to the desired reaction temperature. We used a cylindrical radiant heater, in which we controlled the temperature using a temperature controller.

ESR measurement. We measured the ESR signals using a Bruker EMXplus ESR spectrometer operated at X-band (~9.5 GHz microwave frequency), dual cavities, 100 KHz. We acquired the spectra at room temperature. We used the following operating parameters: microwave power 1mW, attenuation 23.0, modulation amplitude 1G, receiver gain 30 dB, sweep width 100 G, center field 3340 G, time constant 30 *m*s, number of points 10, and sweep time 167.7 s. All spectra were run at least 10 times and averaged. g-Values and radical concentrations were determined using

the Bruker Xenon software from the integration of first derivatives signals compared to the signal for 2,2-di-(4-tert-octylphenyl)-1-picryhydrazyl (DPPH) as the calibration standard. We corrected the g-values using DPPH (g-value=2.0036) for the ESR spectrometer's center field instability. We determined the line width (ΔH_{p-p}) as the difference in the magnetic field of the maximum and minimum peaks of the first-derivative ESR spectra.

Table S1. ESR properties of the EPFRs formed on different NPs and at different conditions.

| EPFRs precursors	Temperature (℃)	g-value	ΔH_{p-p} (Gauss)	ΔH_{p-p} (Gauss)	[EPFR] spins/g
anatase-TiO$_2$ with 1, 2 DCB	25	2.0035	0.32	6.8	3.8×10^{15}
	350	2.0051	2.2	8.8	5.0×10^{17}
anatase-TiO$_2$ with 2-MCP	25	2.0005	0.39	26	6.7×10^{16}
	250	2.0042	0.62	6.8	8.5×10^{16}
	350	2.0044	2.38	6.8	3.2×10^{17}
	450	2.0049	8.62	6.4	3.8×10^{18}
rutile-TiO$_2$ with 2-MCP	250	2.0078	0.42	5.2	3.4×10^{17}
rutile-TiO$_2$ with 1, 2-DCB	250	2.0045	0.90	9.6	2.4×10^{17}
rutile-TiO$_2$ with 1, 2-DCB	350	2.0050	1.60	4.8	1.1×10^{18}
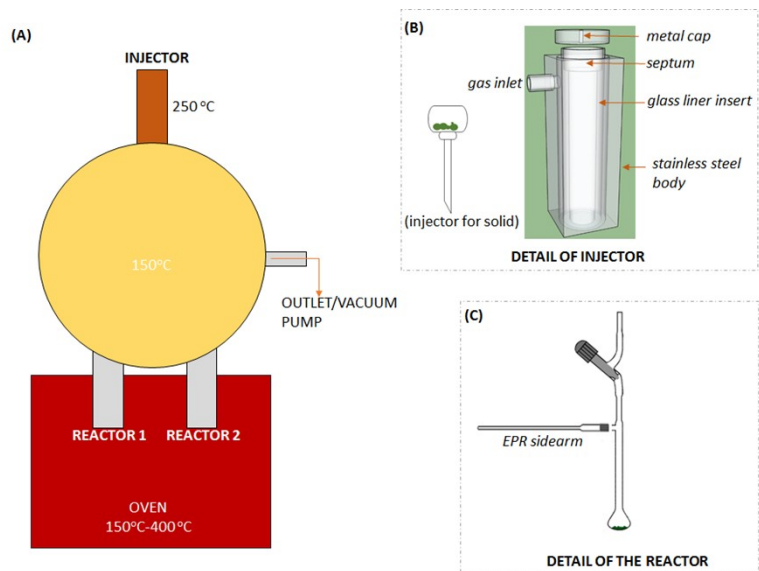
Fig. S1. (A) Thermal reactor for synthesizing EPFRs. **(**B) Detail of the injector and (C) reactor.
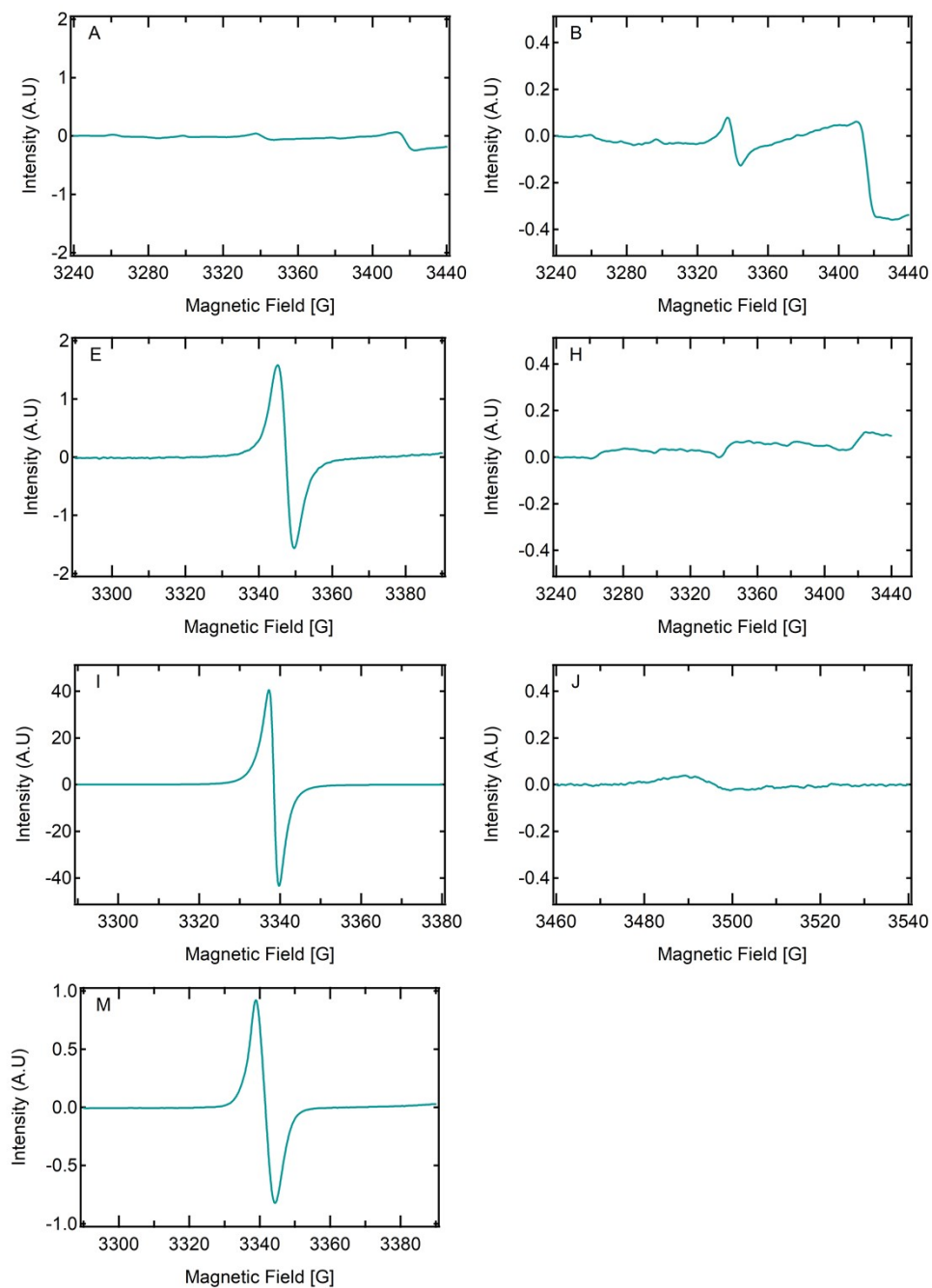
Fig. S2. Representative ESR spectra for conditions A, B, E, H, I, J, and M described in Table 1 for the formation of EPFRs on ZnO at 670 Torr. The plots are on different scales. Panel for condition B is the exact spectra depicted in Fig. 2B but at a wider magnetic field range.
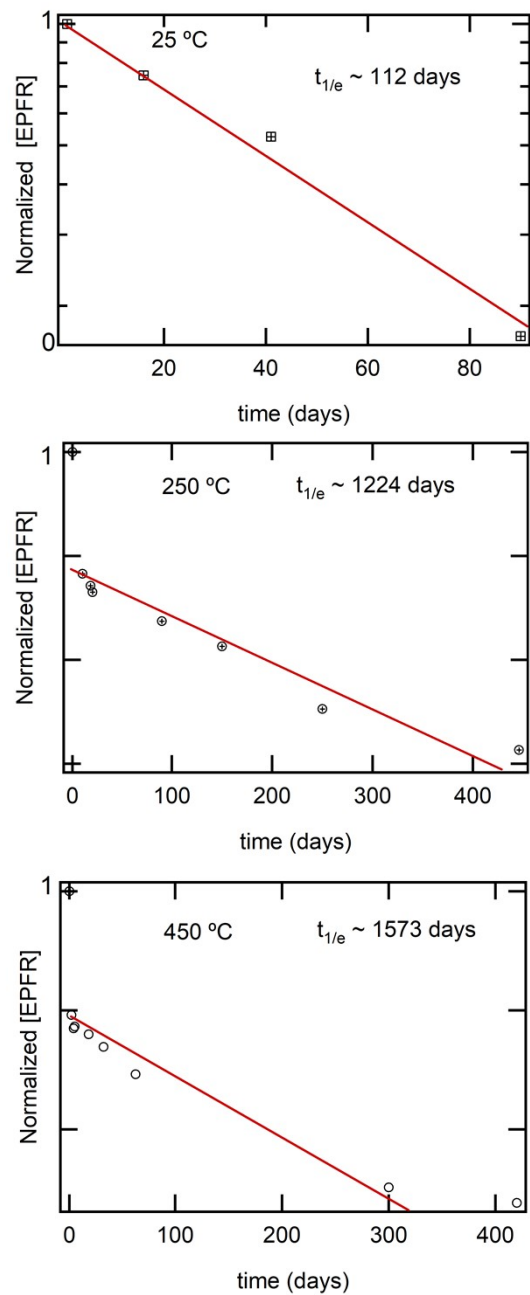
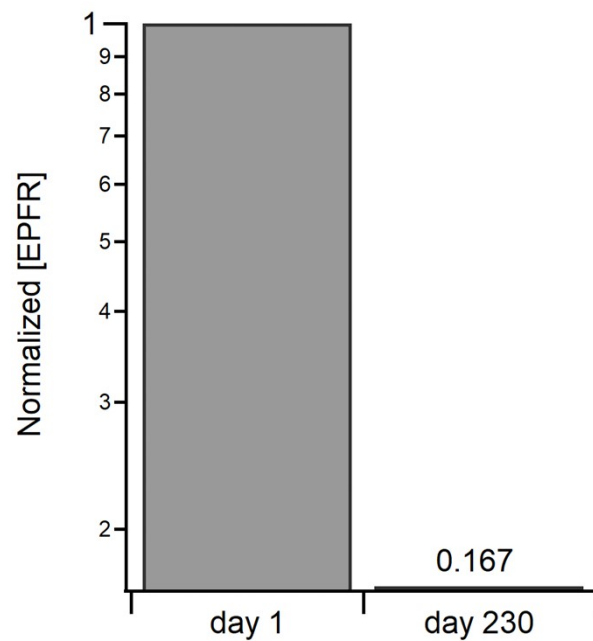**Fig. S3.** Representative time evolution of [EPFR] generated from 2-MCP on anatase-TiO_2.

Fig. S4. Change in the normalized [EPFR] formed on ZnO NPs dosed with 2-MCP at 350 °C after generation and after 230 days of air exposure.
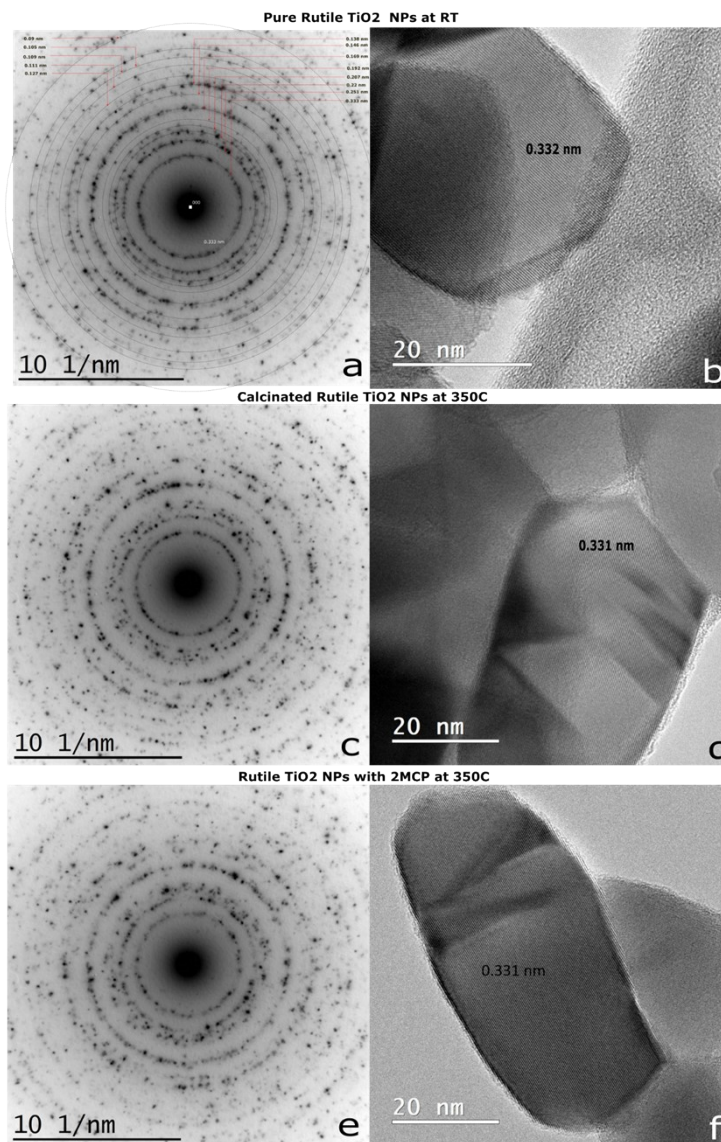
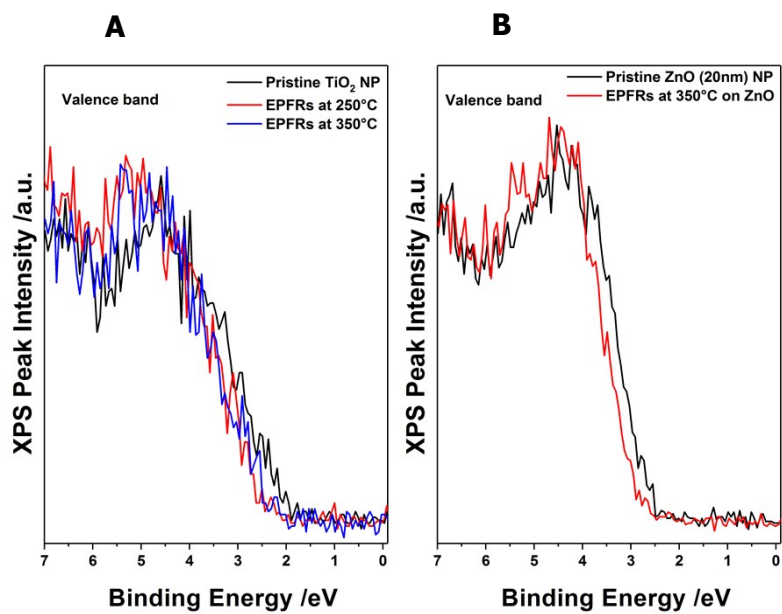**Fig. S5.** Electron diffraction patterns and fringe lines of pure, calcinated, and EPFRs on rutile TiO$_2$ NPs.

Fig. S6. X-ray photoelectron spectra of (A) TiO_2 and (B) ZnO.